AIP Applied Physics Letters

Tailoring the wrinkle pattern of a microstructured membrane

Dong Yan, Kai Zhang, Fujun Peng, and Gengkai Hu

Citation: Applied Physics Letters **105**, 071905 (2014); doi: 10.1063/1.4893596
View online: http://dx.doi.org/10.1063/1.4893596
View Table of Contents: http://scitation.aip.org/content/aip/journal/apl/105/7?ver=pdfcov
Published by the AIP Publishing

APPLIED PHYSICS LETTERS 105, 071905 (2014)

Tailoring the wrinkle pattern of a microstructured membrane

Dong Yan,[1] Kai Zhang,[1,a)] Fujun Peng,[2] and Gengkai Hu[1]
[1]School of Aerospace Engineering, Beijing Institute of Technology, Beijing 100081, China
[2]Aerospace System Engineering Shanghai, Shanghai 201108, China

(Received 11 July 2014; accepted 8 August 2014; published online 19 August 2014)

The realization of controllable wrinkle pattern on a thin membrane is of great importance to micro/nanoengineering and aerospace engineering. Here, we report a straightforward method that achieves this outcome by introducing simple microstructures such as holes into the membrane. For a two-end clamped stretched membrane, the presence of holes redistributes stress field in the membrane, therefore monitors the buckling mode and wrinkle pattern of the membrane. Experiment, numerical simulation, and analytical model are provided to quantify this idea, and several wrinkle patterns are demonstrated. The results can provide insightful ideas to understand wrinkling phenomenon of microstructured membranes and to tailor wrinkle patterns used in various disciplines such as membrane manufacturing, cell differentiation, and film antenna in aerospace engineering. [http://dx.doi.org/10.1063/1.4893596]

Wrinkling is a general phenomenon found in nature,[1–4] and it also occurs in classes of applications in aerospace engineering[5,6] and micro/nanoengineering.[7–14] Tailoring the wrinkle pattern of a membrane may present considerable interests, for example, ordered micro/nanostructures can be formed by buckling a thin film owing to thermal contraction of the underlying substrate,[9–14] offering numerous applications as stretchable electronics.[12–16] Basically, if certain boundary of a membrane is constraint, the membrane tends to wrinkle instead of uniform deformation when external stimuli make the membrane extend or shrink.[17–21] A simple example is the wrinkle formation of a stretched membrane with clamped boundaries.[1,21–24] However, this method provides less flexibility to control wrinkle pattern on the membrane. It is known that material properties could be controlled by designing the microstructures.[25–28] This in fact gives some hints to tailor wrinkle pattern on a membrane by introducing simple microstructures, and this idea will be explored in the following. To make the problem as simple as possible, we consider a two-end clamped membrane with holes, and the wrinkle pattern and its manipulation will be examined by experiment, numerical simulation, and analytical method.

The wrinkle pattern of a uniform polyimide membrane with clamped ends is shown in Fig. 1(a), the sine-shape wrinkles are parallel to the loading direction in the central region of the membrane, consistent with the results reported in previous works.[1,21–24] Then, we consider the effect of a circular hole on the wrinkle pattern of membrane. To keep the symmetry of membrane, a pair of holes with a fixed radius r_0 of 1.5 mm is punched along the central line of the membrane. Because the distance between the pair of holes is very far comparing with the radius of holes, the interaction of the two holes is neglected. As shown in Figs. 1(b)–1(d), three different kinds of wrinkle patterns are observed by varying the position of holes, defined as the distance x_0 from the hole to the clamped end divided by the half-length L of the membrane. When the holes are located near the clamped ends, $x_0/L = 0.05$ in Fig. 1(b), the wrinkle pattern of the membrane is similar to that of the uniform one but with a smaller amplitude at the same strain level. As x_0/L increases to 0.15, the whole membrane almost remains flat, except a local and small region near the holes [Fig. 1(c)]. When the holes are far from the clamped ends, for example, x_0/L reaches to 0.40 as shown in Fig. 1(d), a different wrinkle pattern takes place, i.e., the most part of the membrane appears to wrinkle except a region between two holes.

In order to understand the wrinkle pattern shift with the changing position of holes, numerical eigenvalue buckling and postbuckling analysis are carried out by using the commercial finite element software ABAQUS. The shell element S4R and linear elastic constitutive model are used.[29] The geometric parameters and material properties used in the numerical simulation are the same as those in the experiment. A mesh sensitivity study is performed to ensure that the element sizes are sufficiently fine. The numerical simulations on the membranes in Fig. 1 by postbuckling analysis agree well with the experimental results, demonstrating that the

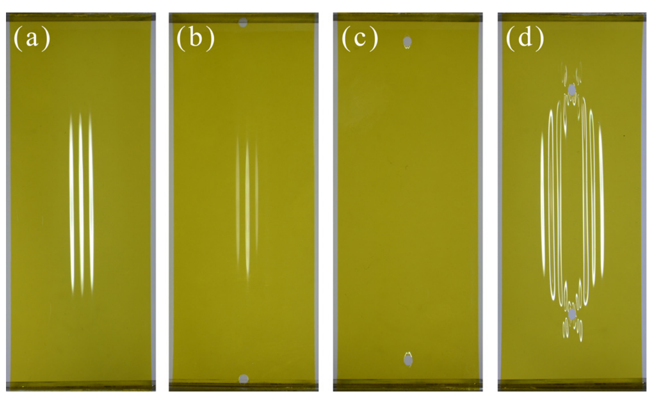

FIG. 1. Wrinkle patterns of a two-end clamped stretched membrane (width-length ratio $\lambda = 0.4$) at 5% strain observed in experiment: (a) membrane without holes, membrane with holes at (b) $x_0/L = 0.05$, (c) $x_0/L = 0.15$, and (d) $x_0/L = 0.40$.

a)Author to whom correspondence should be addressed. Electronic mail: zhangkai@bit.edu.cn

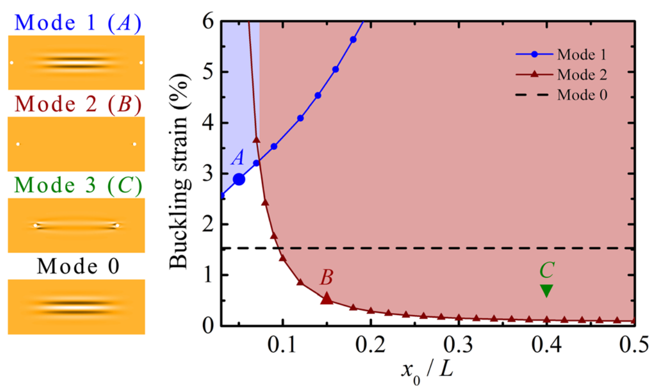

FIG. 2. Buckling modes and corresponding buckling strains versus the position of holes. The points A, B, and C correspond to specimens shown in Figs. 1(b)–1(d), respectively.

observed different wrinkle patterns are the result of buckling of the membrane with holes.[29] By varying the position of holes with a fixed radius r_0, three buckling modes and corresponding buckling strains are plotted in Fig. 2 by eigenvalue buckling analysis. When the holes are located near the clamped ends (blue region), the membrane will deform into the lowest buckling mode of the sine-shape pattern (mode 1), which is similar to that of the uniform membrane (mode 0). The critical buckling strain of the membrane increases with rising distance x_0/L until to 0.072. With further increase of x_0/L (red region), a turnover happens, i.e., the lowest buckling mode will transform from mode 1 into mode 2, in which wrinkles only decorate the local region near the holes. When the holes are far from the clamped ends, e.g., $x_0/L = 0.40$, the higher buckling mode, mode 3, occurs at the strain level close to that of mode 2. As a result, the wrinkle pattern may mix modes 2 and 3 (or other higher modes) at a relative low strain level, as proved by our experiment [Fig. 1(d)] and postbuckling analysis.[29] It is also observed that the critical buckling strain of the membrane with holes is significantly higher than that of the uniform membrane when x_0/L is less than 0.096, suggesting an increase of the membrane stability. Although people have studied the wrinkles around holes in substrates,[9,10] as well as elastic sheets with holes,[19] the disappearance of wrinkle controlled by putting two holes in a free-standing sheet has not been reported.

Now we are ready to explain the observed wrinkle patterns in terms of the stress distribution on the membrane by developing an analytical model. The basic idea is the following: According to previous works,[1,21,22] the deforming process of a stretched membrane under clamped boundaries can be divided into two parts, a uniform uniaxial tension force is first introduced to stretch the membrane and then a shear force is provided to prevent the contraction due to the clamped end. For simplification, a pair of concentrated forces F is used to replace the nonuniform distributed shear force on the clamped end.[29] By assuming the solution in the form of a Fourier series,[30] the analytical stress of a two-end clamped uniform membrane under stretched strain ε_x can be obtained as

$$
\begin{aligned}
\sigma_x &= E\varepsilon_x + \frac{2F}{L}\sum_{m=1}^{\infty}\left[\left(A - \frac{B}{m_\lambda}\right)\cosh(m_\lambda y_r) - B y_r \sinh(m_\lambda y_r)\right]\cos\left(\frac{m_\lambda}{\lambda}x_r\right),\\
\sigma_y &= \frac{F}{L} - \frac{2F}{L}\sum_{m=1}^{\infty}\left[\left(A + \frac{B}{m_\lambda}\right)\cosh(m_\lambda y_r) - B y_r \sinh(m_\lambda y_r)\right]\cos\left(\frac{m_\lambda}{\lambda}x_r\right),\\
\tau_{xy} &= \frac{2F}{L}\sum_{m=1}^{\infty}\left[A \sinh(m_\lambda y_r) - B y_r \cosh(m_\lambda y_r)\right]\sin\left(\frac{m_\lambda}{\lambda}x_r\right),\\
A &= (-1)^m \frac{-m_\lambda \cosh m_\lambda}{\cosh m_\lambda \sinh m_\lambda + m_\lambda},\\
B &= (-1)^m \frac{-m_\lambda \sinh m_\lambda}{\cosh m_\lambda \sinh m_\lambda + m_\lambda},
\end{aligned}
\tag{1}
$$

where $x_r = x/L$ and $y_r = y/C$ are the coordinates along the length $2L$ and width $2C$ direction, respectively, with the origin at the center of the membrane. $\lambda = C/L$ is the width-length ratio and $m_\lambda = m\pi\lambda$. The concentrated force $F = \alpha\nu\varepsilon_x EC$, and α is a factor related to the equivalence between the concentrated force and the nonuniform distributed shear force, which keeps nearly constant 0.38 for slender membranes ($\lambda \le 0.45$). E and ν are the Young modulus and Poisson ratio of the membrane, respectively. Our analytical solution has rapid convergence performance and high accuracy for slender membranes except small regions near the boundaries.[29] Similarly, when the hole is much smaller comparing with the size of membrane, the stress solution of an infinite plate with a circular hole under uniform tension[30] and the analytical stress solution in Eq. (1) can be adopted to describe the stress distribution of a stretched membrane with holes.[29] Furthermore, effective force F_y, defined as the integral of σ_y with respect to y from $-C/2$ to $C/2$, can be used to analyze the mechanism of buckling together with local stress field because of the high compressive stress near the holes.

Figure 3 shows the results of F_y and σ_y for the membranes in Fig. 1. As shown in Fig. 3(b), when the membrane is stretched with the clamped ends, there are tensile region near the clamped ends and compressive region in the center of the membrane. But the trend is reversed for the stress caused by the hole along the central line of the membrane, i.e., a remarkable compressive region near the hole and a tensile region relatively far from the hole.[29] So variation on the

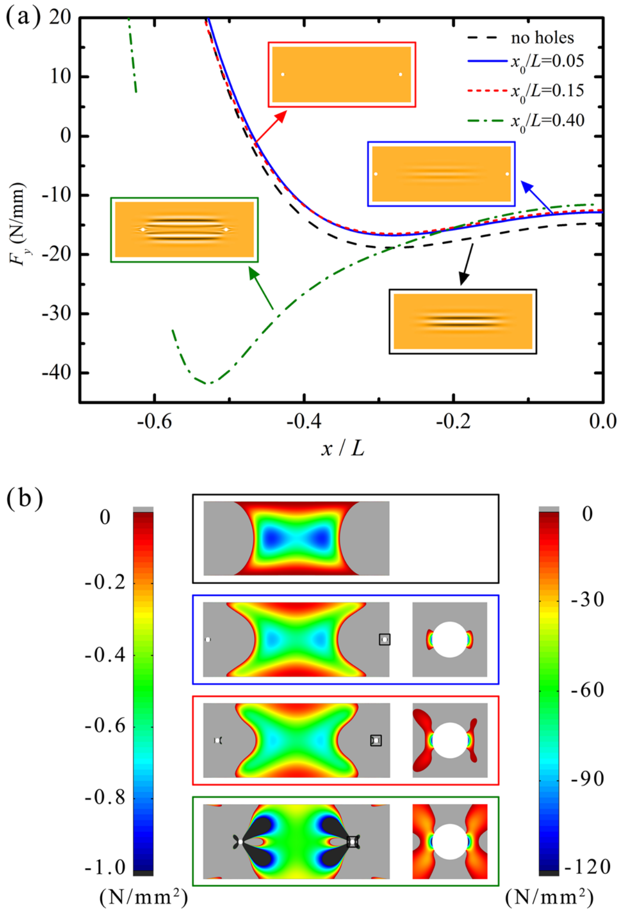

FIG. 3. Analytical stress analysis of the stretched membrane with the variation on the position of holes at 5% strain: (a) effective force F_y and (b) σ_y of the membrane. Only the left half of F_y is plotted due to the symmetry.

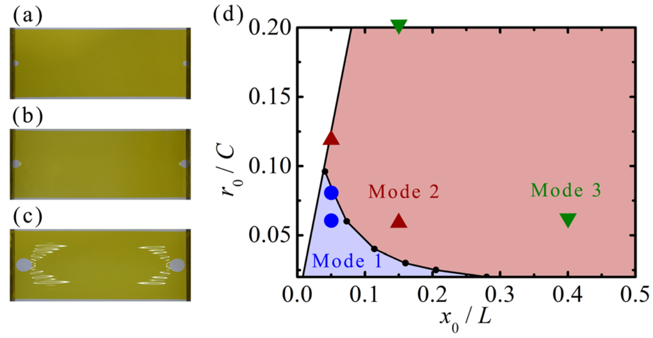

FIG. 4. Wrinkle patterns of a stretched membrane with holes at 5% strain. The radius r_0 and distance x_0/L are (a) 2.0 mm and 0.05, (b) 3.0 mm and 0.05, and (c) 5.0 mm and 0.15, respectively. (d) Phase diagram of wrinkle pattern related to the position and radius of holes. According to the position and radius of holes, the six specimens in experiment shown in Figs. 1(b)–1(d) and Figs. 4(a)–4(c) are marked by the big symbols.

position of holes will lead to different superposition results. For example, as shown in Fig. 3(a), when the holes are located near the clamped ends, the compressive force in the center of the membrane decreases due to the introduced tensile force caused by the holes. As a result, the membrane will have a higher critical buckling strain and a smaller amplitude of the wrinkle. As increasing x_0/L, the compressive force in the center of the membrane decreases further, even resulting in vanishing of the wrinkles on membrane at the same strain level; however, the region near the holes endures a large compressive stress and thus becomes easy to buckle. Mode 2 will be therefore triggered instead of mode 1. When the holes are punched near the region of compressive force, a remarkable increase of compressive force and region in the membrane can trigger the mixed pattern of modes 2 and 3 (or other higher modes). In addition, there are obvious tensile regions between two holes, which is the reason why a flat region between two holes is observed in Fig. 1(d).

Actually, not only the position of holes but also the radius of holes can trigger the transformation of wrinkle patterns, which has been observed by experiment (Fig. 4) and numerical postbuckling analysis.[29] The membrane in Fig. 4(a) is little wrinkled. Comparing with the pattern in Fig. 1(b), the larger holes can provide larger tensile stress to neutralize the compressive stress in the membrane, and therefore reduce the amplitude of wrinkle. However, as the increasing radius of holes, the holes lead to a remarkable increase of compressive force and region in the membrane, and the distance x_0/L should be changed to achieve the expected wrinkle pattern. Meanwhile, when the distance x_0/L is fixed, the radius of holes also needs to be chosen properly. For example, when the distance x_0/L is fixed at 0.15, the holes with r_0 equal to 1.5 mm can eliminate the wrinkles on membrane [Fig. 1(c)], but increasing r_0 up to 5.0 mm will make the wrinkles serious [Fig. 4(c)]. A phase diagram of wrinkle pattern related to the position and radius of holes is given in Fig. 4(d) by numerical eigenvalue buckling analysis, indicating that the wrinkle pattern could be controlled by designing the position and radius of holes.

Furthermore, effective control of the wrinkle pattern can also be achieved by designing the distribution of holes. As shown in Fig. 5, when holes with a radius of 2.0 mm are arranged in square and hexagonal patterns, some local wrinkles will be formed near the holes with the same pattern as the arrangement of holes. The local wrinkles near a single hole are the mixed pattern of mode 2, mode 3, and other higher modes (Fig. 2). The wrinkles of the microstructured membrane with periodic-arranged large holes can be regarded as the collection of the wrinkle pattern of a single

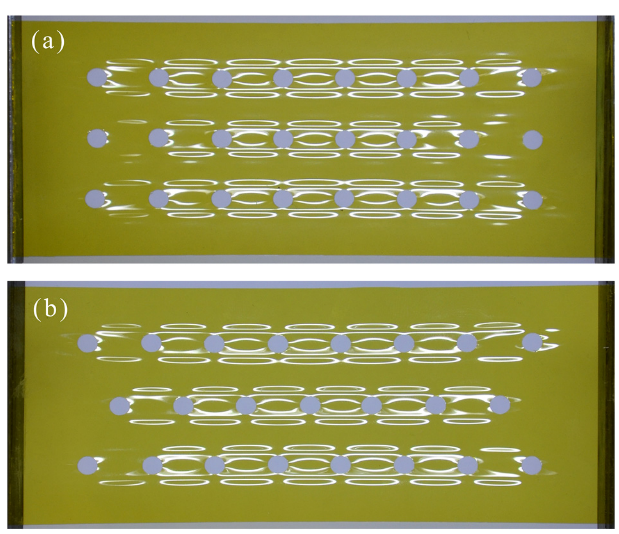

FIG. 5. Wrinkle patterns achieved by designing the distribution of holes: holes with a radius of 2.0 mm are arranged in square pattern (a) and hexagonal pattern (b).

hole. Hence, wrinkle pattern of the membrane would have a significant dependence on the distribution of holes.

Actually, besides the wrinkling of a two-end clamped membrane under tension, many soft material systems perform morphological instability and surface wrinkling under various environmental stimuli, e.g., wrinkling of a stiff film anchored by a compliant substrate and surface wrinkling on a core-shell soft sphere.[9–14,20] For these systems, elastic instability is often triggered when large enough compressive stress is generated in materials due to inhomogeneous deformation or constrained swelling/growing.[14] Our proposed perforating method should also be available in other systems to tailor tunable wrinkle patterns effectively. In previous works,[9,10] wrinkle patterns of a stiff film anchored by a compliant substrate have been controlled by patterning the surface of substrate. In this model, the non-uniform compressive stress generated by the structural heterogeneity of patterned substrate is applied on the stiff film and triggers regular wrinkles.[9,10] In contrast, designing the microstructures of film by perforating method, such as punching large holes on the film, can redistribute the stress field in the film and motivate different wrinkles. Furthermore, the wrinkle pattern and its wavelength strongly depend on the material properties, which can be changed by introducing holes in periodic arrangement.

We have observed wrinkle patterns in a stretched membrane with holes. We also show the ability to control these wrinkle patterns by designing microstructures of the membrane such as varying the position, radius, and distribution of holes. The effect has been revealed at millimeter scale but should also be at work at micro or even smaller scales. There are considerable current interests in developing complex pattern of surface wrinkles for applications in sensors,[12,13,15] optical components,[13,15] templates with complex ordered structures,[12,13] or morphology and differentiation of cell.[8] Our work offers a potential method to produce targeted surface wrinkles with tailored pattern. Equally important, thin membranes for use sometimes demand very smooth surfaces with few wrinkles such as film antenna in aerospace engineering. Our work indicates that wrinkles can be eliminated in a stretched membrane by introducing properly designed holes.

To conclude, we have investigated wrinkle pattern formation of a stretched microstructured membrane by designing the microstructures, including varying the position, radius, and distribution pattern of holes. It is found that the microstructures such as holes can make the membrane display a desired wrinkle pattern or even a suppression of wrinkles in a stretched membrane. The mechanism of the different wrinkle patterns is due to the modification of stress field in the membrane by introducing microstructures, resulting in variations on the buckling mode and wrinkle pattern of the membrane. Our study provides a simple and effective method to control and design wrinkle patterns of a membrane and may be applied in various disciplines such as membrane manufacturing, cell locomotion, and aerospace engineering.

We thank Shaopeng Ma, Qinwei Ma, and Xian Wang for the help in experiment. Supports from NSFC (Grant Nos. 11202025 and 11290153) and SAST (Grant No. 201253) are acknowledged.

[1]E. Cerda and L. Mahadevan, Phys. Rev. Lett. **90**, 074302 (2003).
[2]E. Cerda, J. Biomech. **38**, 1598 (2005).
[3]T. Savin, N. A. Kurpios, A. E. Shyer, P. Florescu, H. Liang, L. Mahadevan, and C. J. Tabin, Nature **476**, 57 (2011).
[4]H. Liang and L. Mahadevan, Proc. Natl. Acad. Sci. U.S.A. **106**, 22049 (2009).
[5]J. R. Blandino, J. D. Johnston, and U. K. Dharamsi, J. Spacecr. Rockets **39**, 717 (2002).
[6]Y. W. Wong and S. Pellegrino, J. Mech. Mater. Struct. **1**, 3 (2006).
[7]A. K. Harris, P. Wild, and D. Stopak, Science **208**, 177 (1980).
[8]M. Guvendiren and J. A. Burdick, Biomaterials **31**, 6511 (2010).
[9]N. Bowden, S. Brittain, A. G. Evans, J. W. Hutchinson, and G. M. Whitesides, Nature **393**, 146 (1998).
[10]W. T. S. Huck, N. Bowden, P. Onck, T. Pardoen, J. W. Hutchinson, and G. M. Whitesides, Langmuir **16**, 3497 (2000).
[11]Z. Y. Huang, W. Hong, and Z. Suo, J. Mech. Phys. Solids **53**, 2101 (2005).
[12]S. Singamaneni and V. V. Tsukruk, Soft Matter **6**, 5681 (2010).
[13]Y. Mei, S. Kiravittaya, S. Harazim, and O. G. Schmidt, Mater. Sci. Eng., Rep. **70**, 209 (2010).
[14]B. Li, Y. P. Cao, X. Q. Feng, and H. Gao, Soft Matter **8**, 5728 (2012).
[15]J. A. Rogers, T. Someya, and Y. Huang, Science **327**, 1603 (2010).
[16]Y. Su, J. Wu, Z. Fan, K. C. Hwang, J. Song, Y. Huang, and J. A. Rogers, J. Mech. Phys. Solids **60**, 487 (2012).
[17]J. W. Wang, Y. P. Cao, and X. Q. Feng, Appl. Phys. Lett. **104**, 031910 (2014).
[18]J. Hure, B. Roman, and J. Bico, Phys. Rev. Lett. **109**, 054302 (2012).
[19]M. Taylor, K. Bertoldi, and D. J. Steigmann, J. Mech. Phys. Solids **62**, 163 (2014).
[20]B. Li, F. Jia, Y. P. Cao, X. Q. Feng, and H. Gao, Phys. Rev. Lett. **106**, 234301 (2011).
[21]E. Cerda, K. Ravi-Chandar, and L. Mahadevan, Nature **419**, 579 (2002).
[22]N. Friedl, F. G. Rammerstorfer, and F. D. Fischer, Comput. Struct. **78**, 185 (2000).
[23]V. Nayyar, K. Ravi-Chandar, and R. Huang, Int. J. Solids Struct. **48**, 3471 (2011).
[24]V. Nayyar, K. Ravi-Chandar, and R. Huang, Int. J. Solids Struct. **51**, 1847 (2014).
[25]Y. Su, B. Ji, K. Zhang, H. Gao, Y. Huang, and K. C. Hwang, Langmuir **26**, 4984 (2010).
[26]K. Zhang, H. Duan, B. L. Karihaloo, and J. Wang, Proc. Natl. Acad. Sci. U.S.A. **107**, 9502 (2010).
[27]K. Bertoldi, P. M. Reis, S. Willshaw, and T. Mullin, Adv. Mater. **22**, 361 (2010).
[28]X. N. Liu, G. K. Hu, G. L. Huang, and C. T. Sun, Appl. Phys. Lett. **98**, 251907 (2011).
[29]See supplementary material at http://dx.doi.org/10.1063/1.4893596 for the details on experiment, numerical simulation, and analytical model.
[30]S. P. Timoshenko and J. N. Goodier, *Theory of Elasticity* (McGraw-Hill Book Company, Tokyo, 1970).